

See discussions, stats, and author profiles for this publication at: <https://www.researchgate.net/publication/276882696>

Polymer electrolytes—relaxation and transport properties

ARTICLE *in* IONICS · APRIL 2014

Impact Factor: 1.75 · DOI: 10.1007/s11581-014-1256-3

READS

17

2 AUTHORS, INCLUDING:



Chin Han Chan

Universiti Teknologi MARA

41 PUBLICATIONS **160** CITATIONS

SEE PROFILE

Polymer electrolytes—relaxation and transport properties

Chin Han Chan · Hans-Werner Kammer

Received: 23 June 2014 / Revised: 13 August 2014 / Accepted: 14 September 2014 / Published online: 15 October 2014
© Springer-Verlag Berlin Heidelberg 2014

Abstract Relaxations in polymer electrolytes were studied in poly(ethylene oxide) and epoxidized natural rubbers both filled with lithium perchlorate. Impedance relaxation was investigated over a wide range of salt concentration at room temperature. Imaginary part of impedance as a function of frequency exhibits generally one maximum and one minimum. These two extreme values rule properties in the DC limit. They can be related to transport properties and degree of dissociation. It turns out that DC conductivity is dominantly ruled by transport coefficient.

Keywords Dielectric impedance · Transport coefficient · Epoxidized natural rubber · Poly(ethylene oxide)

Introduction

Polymer electrolytes are mixtures of an organic polymer and an inorganic salt. These systems attracted intensive research activities in the last decades [1–12]. This paper is a continuation of our previous contribution to polymer electrolytes [13]. There are quite a number of studies dealing with electrolytes comprising poly(ethylene oxide) (PEO), where the molecular mass of PEO ranges mostly below the entanglement molecular mass [14, 15]. In what follows, we report about the variation of properties with salt content in

polymer-salt mixtures with polymers having molecular masses above entanglement molecular mass.

Mixtures of PEO and epoxidized natural rubber (ENR) (i.e., 25 and 50 mol% of epoxide content) with lithium perchlorate (LiClO_4) salt were studied. There are quite a number of studies dealing with PEO-based electrolytes [14, 16–21]; On the other hand, works on ENR-based polymer electrolytes are scant [8, 22]. Enhancement of conductivity for immiscible blends of PEO/ENR polymer electrolytes as compared to neat PEO at comparable salt content is observed [6, 23–27]. However, conduction mechanism of the parent polymers and the blends with addition of Li salt is not well scrutinized in those studies except that hints on preferential solubility of Li salt in the PEO phase of the blends were discussed in [6, 23, 27]. Interaction of Li salts with PEO and ENR by Fourier-transform infrared spectroscopy [23, 28], morphological studies by polarizing optical microscopy of PEO polymer electrolytes [7], and the increase in rigidity of the PEO chains with addition of Li salt [21] were reported as well.

From an electric point of view, one may say polymer-salt systems consist of conductive and dielectric regions. The regions form a random and periodic network of resistors and capacitors or of resistor-capacitor (RC) circuits. Accordingly, the real part of complex conductivity displays its frequency dependence in the region below 1 MHz. Here, we want to illuminate the DC limit. Thereby, we focus on two frequency regions characterized by different values of $\omega=(RC)^{-1}$. Under ideal conditions, capacitors do not play a prominent role in the low-frequency range. Conductivity approaches DC conductivity which is ruled by the resistor of the system and reflected in real part of impedance as frequency-independent range. In real systems, however, electrode polarization cannot be neglected. In addition to bulk capacitor (C_f) of the polymer-electrolyte film, we have double-layer capacitors (C_{dl}), at the interfaces electrode-electrolyte with C_{dl}

C. H. Chan (✉) · H.-W. Kammer
Faculty of Applied Sciences, Universiti Teknologi MARA,
40450 Shah Alam, Selangor, Malaysia
e-mail: cchan_25@yahoo.com.sg

C. H. Chan
e-mail: cchan@salam.uitm.edu.my

H.-W. Kammer
Department of Chemistry and Physics, Martin Luther University of
Halle-Wittenberg, 06099 Halle, Saale, Germany

C_f . As a result, the low-frequency range or the DC limit is characterized by

$$(RC_{dl})^{-1} = \omega_{\min} \quad (1)$$

With increasing frequency, the AC response consists of comparable contributions of film resistor and capacitor. The imaginary part of impedance displays a maximum at

$$\omega_{\max} = (RC_f)^{-1} \quad (2)$$

These two frequencies are provided by impedance spectroscopy and form prominent characteristics for determination of transport properties of charge carriers and degree of dissociation of charge carriers in polymer electrolytes.

Impedance studies in variation of salt concentration of polymer electrolytes were reported by other groups [12, 16, 29]. In a lot of cases, discussion of electrical modulus (M) [29, 30], which can be related to the viscoelastic relaxation, were attempted. Here, the impedance (Z) is the most basic unit. The curves of the imaginary part (Z'') and the real part (Z') of the impedance as a function frequency shows Z' and Z'' cross closely to $Z' = 0.5R_b$ if the ion relaxation closes to Debye relaxation. R_b denotes bulk DC electrolyte resistance. This can be easily seen in this scheme, but not as easy in plots of imaginary part of the electrical modulus as a function of frequency.

In this paper, we intend to elucidate the approaches for the determination of transport properties of charge carriers and the degree of dissociation of charge carriers in polymer electrolytes, which sketched briefly in the “Theoretical Background and Results and Discussion” section. Results are discussed in terms of these approximations. The scheme proposed is applicable to other polymer electrolytes.

Experimental

LiClO_4 was added to PEO and ENRs with two epoxidation levels. Details to materials, preparation of samples, and impedance spectroscopy are given elsewhere [9] but are reported briefly in this section.

Materials

PEO and ENR- x were supplied by Sigma-Aldrich Chemical Co. (St. Louis, MO, USA) and Malaysian Rubber Board (Sungai Buloh, Malaysia), respectively. ENR- x denotes epoxidized natural rubber with $x\text{mol}\%$ of epoxy content. LiClO_4 (Acros Organics Co., Geel, Belgium) was added to the polymers. The characteristics of polymers and salt are listed in

Table 1. PEO was purified before further use by dissolution in chloroform (CHCl_3 , Merck, Darmstadt, Germany) and precipitation in n -hexane (Merck, Darmstadt, Germany). ENR-25 and ENR-50 were dissolved in chloroform, followed by the removal of cross-linked gel by filtration and then precipitation in methanol. LiClO_4 was used without further purification where it was dried in the vacuum oven for 24 h at 120 °C.

Preparation of samples

Solution casting technique was used to prepare the solid thin films of polymer electrolytes. Solvents of tetrahydrofuran (THF) (Merck, Darmstadt, Germany) (for rubbers) and methanol (CH_3OH) (Merck, Darmstadt, Germany) (for PEO) were kept dry by addition of molecular sieves with a pore diameter of 3 Å from Merck, Darmstadt, Germany. Different concentrations of LiClO_4 were added to 2 % w/w of polymer stock solution in THF or CH_3OH . The mixture was stirred at 50 °C for 48 h and was poured slowly into a Teflon dish. The casting of the mixture into the Teflon dish was done very carefully in order to avoid forming any bubbles on the surface of the solution. Polymer film was dried for 24 h for rubbers and 1 h for PEO at 80 °C under nitrogen gas purging before further drying in a vacuum oven for 24 h at 50 °C. Dried polymer film was stored in desiccators. Approximately 24 h before analysis by impedance spectrometer (IS), the sample was dried again in the vacuum oven at 50 °C for 24 h.

Table 1 Characteristics of the polymers

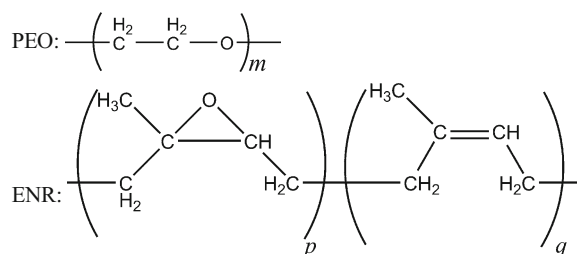
	PEO	ENR-25	ENR-50
$M_n^a/\text{kg mol}^{-1}$	300		
$M_w^b/\text{kg mol}^{-1}$		1,060	700
$M_n^b/\text{kg mol}^{-1}$		381	200
$T_g/^\circ\text{C}$	−54	−42	−21
$M_{\text{repeat unit}}/\text{g mol}^{-1}$	44	72	76
$\rho/\text{g cm}^{-3}$	1.2 ^c	0.97 ^d	1.03 ^d

^a Viscosity-average molecular weight provided by the supplier

^b Weight- and number-average of molecular weight as estimated in this work by Agilent gel permeation chromatography (GPC). Polystyrene with low polydispersity was used as standard

^c Density of PEO adopted from [4]

^d Density of rubbers adopted from [31]



For ENR-25: $p = 0.75$, $q = 0.25$; ENR-50: $p = 0.5$, $q = 0.5$

Impedance analysis

Ionic conductivity (σ_{AC}) at roughly 25 °C was determined from AC-impedance measurement using a Hioki 3532-50 LCR HiTester impedance spectroscopy (Hioki, Nagayo, Japan) interfaced with a computer for data acquisition over the frequency (f) range between 50 to 1 MHz. Film of polymer electrolyte was sandwiched between two stainless steel disk electrodes, which acted as blocking electrodes for ions. Quantity σ_{DC} was calculated from the bulk DC electrolyte resistance (R_b) by adopting equation $\sigma_{DC}=L/(R_b \cdot A)$. Quantities L and A denote thickness of the polymer electrolyte film and its surface area in contact with the stainless steel disk electrodes. The diameter of the electrode is 20 mm. The average of thickness L was determined from three measurements of thickness on the dry polymer film at three different positions that were in contact with the stainless steel disk electrodes. Thickness was measured by the use of Mitutoyo Digimatic Caliper (Mitutoyo Corp., Kanagawa, Japan). The thickness of the solid films is in the range of 0.25–0.40 mm. Quantity σ_{DC} was either estimated from Cole-Cole plots or from the values of real and imaginary parts of impedance at angular frequency for fully stabilized network [$Z'(\omega_o)$] and [$Z''(\omega_o)$] at maximum of Z'' (as discussed in [13]). The averages of Z' and Z'' were used after four to five impedance analyses with errors of σ_{DC} approximately at 10 %.

Gel permeation chromatography

The weight-average (M_w) and number-average (M_n) molecular weight of neat polymer were estimated by gel permeation chromatography (GPC) at 40 °C using an Agilent 1200 GPC (Agilent Technologies Inc., Santa Clara, CA, USA) coupled with refractive index detector and Waters Styragel Columns HR 3, and HR 5E. HPLC grade of CHCl_3 (Thermo Fisher Scientific, Loughborough, UK) was used as eluent at flow rate of 0.8 mL min^{-1} and solvent with sample concentration of 1.0 mg mL^{-1} . Polystyrene standards (Sigma-Aldrich, St. Louis, MO, USA) ($M_w=70,000$ to $1,000,000 \text{ g mol}^{-1}$) with low polydispersity were used to prepare a calibration curve.

Theoretical background and results and discussion

Relaxation and transport

Important experimental information from impedance spectroscopy is given by the following data: DC resistance (R_b), frequencies ω_{\max} and ω_{\min} where imaginary part of impedance $Z''(\omega)$ displays extreme values. These frequencies serve for characterization of the DC limit. Relationships are given in Eqs. (1) and (2). Ohm's resistance governs DC conductivity,

$\sigma_{DC}=L/(R_b \cdot A)$ with sample thickness and area, L and A , respectively.

DC conductivity is ruled by the density of charge carriers and their mobility. It reads for a 1:1 electrolyte as LiClO_4

$$\sigma_{DC}=e \frac{N_{+}}{v} (\mu_{+}+\mu_{-})=\frac{F^2}{RT} D_{\text{ion}} C_S \quad (3)$$

where N_{+}/v denotes the number of cations per volume and μ_{\pm} is the ion mobility. The latter has been simplified to mean ionic mobility and replaced in the last equation by diffusion coefficient (D_{ion}) via Nernst-Einstein relationship with Faraday constant, $F=eN_A$, and molar concentration of dissociated or polarized molecules, $C_S=\frac{N_{\pm}}{N_A v}$. Equation (3) demonstrates for a polymer electrolyte, and measurement of conductivity σ_{DC} yields only the product $D_{\text{ion}} \cdot C_S$. In other words, neither D_{ion} nor C_S refers to free charge carriers but to charge carriers coupled to polymer chains. Quantity $D_{\text{ion}} \cdot C_S$ gives the motion of charges or dipoles per length scale. In that sense, after Eq. (3), quantity D_{ion} describes the random walk of charge carriers coupled to polymer chains in DC limit. For an illustration of this situation, Fig. 1 presents impedance versus frequency for a mixture of PEO and Li salt, where the concentration of salt is given by $Y_S=(\text{mass of salt})/(\text{mass of polymer})$. One recognizes that the minimum in reduced imaginary part (Z''/R_b) coincides with $Z'=R_b$, which signals DC conductivity plateau. At still lower frequencies, both Z' and Z'' increase due to electrode polarization. Hence, we may approximate the length scale, characterizing $D_{\text{ion}} \cdot C_S$, by thickness of the diffuse double layer at the electrode-electrolyte interface. In other words, $Z''(\omega)$ displays the

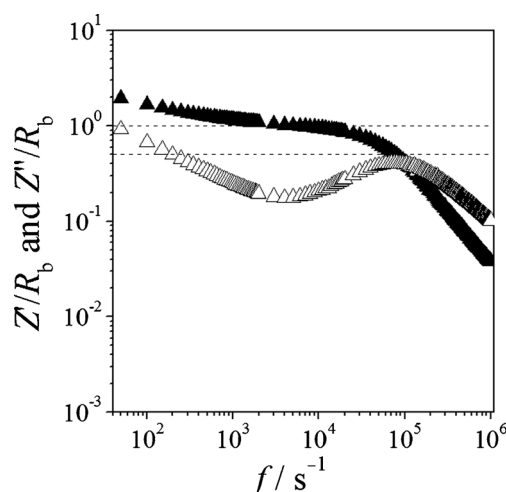


Fig. 1 Real (solid marker) and imaginary (open marker) part of reduced impedance for PEO filled with LiClO_4 at room temperature; $Y_S=0.1$

minimum at low frequencies which is governed by double-layer capacitor or electrode polarization. The ratio of film and double-layer capacitor might be simply expressed by the ratio of corresponding thicknesses, $C_f/C_{dl}=l/L$. It is approximately given by the ratio of the two frequencies characterizing Z'' , $(\omega_{\min}/\omega_{\max})^2$. As a result, motion of charge carriers in the DC limit can be characterized by

$$l^2 = D_{\text{ion}}\tau_{\min} \quad (4)$$

where l gives the thickness of the double-layer capacitor and $\tau_{\min}=\omega_{\min}^{-1}$. Having stipulated the length scale, Eq. (4) allows for determination of D_{ion} and subsequently estimation of C_S after Eq. (3).

One may also reformulate Eq. (3) in terms of added salt concentration (C_S^*) to the polymer. Then, conductivity appears proportional to the product of the ratio of concentrations α and D_{ion} . It follows

$$\sigma_{\text{DC}} \propto (\alpha D_{\text{ion}}) C_S^* \text{ with } \alpha \equiv \frac{\Lambda^*}{\Lambda} = \frac{C_S}{C_S^*} \quad (5)$$

where Λ symbolizes the respective equivalent molar conductivity. Quantity α might be seen as degree of dissociation of salt in the polymer electrolyte. Details for determination of diffusion coefficient and degree of dissociation are summarized in the “Appendix” section.

Diffusion coefficient and degree of dissociation

Figure 1 displays extreme values of imaginary part of impedance $Z''(f)$. Salt content (Y_S) acts as parameter. In the low-frequency limit, $\omega \rightarrow 0$, one observes

$$\frac{Z'}{R_b} \rightarrow 1 \text{ and } \frac{Z''}{R_b} \rightarrow 0 \text{ if } \frac{C_f}{C_{dl}} = 0 \quad (6)$$

For $C_f/C_{dl} > 0$, however, one finds dipolar relaxation in the same limit (cf. Eq. (18))

$$\frac{Z'}{R_b} = 1 + \frac{\text{const}}{\omega^n} \text{ and } \frac{Z''}{R_b} = \frac{\text{const}}{\omega^n} \text{ with } n < 1 \quad (7)$$

The example of Fig. 1 shows increase of impedance with descending frequency after the indicated power law with $n=0.51$. The combination of relationships (6) and (7) reveals that function $Z''(\omega)$ displays a minimum when $C_f/C_{dl} > 0$. Moreover, a relaxation peak is observed for the conductivity-related quantity Z'' . Extreme values of Z''/R_b reveal relaxations of

segments under influence of charge carriers. These relaxations promote mobility of dipoles or ions. Therefore, the interaction between salt and chain molecules generates varying conductivity in polymer electrolytes. We note that frequency of minimum as well as of maximum, displayed by Z'' , increases with increasing salt content. In other words, time constant for segment relaxation decreases under the influence of salt. It is well-known that chain mobility is hampered with increasing salt content as increase of glass transition temperatures (T_g) shows under these conditions [9, 12, 13], an effect which might retard conductivity near T_g [32, 33]. Shift of extreme values in Z'' to higher frequencies with increasing salt content, on the other hand, reflects faster segment relaxation. This effect enhances conductivity [13].

We observe two extreme values in Z''/R_b -spectrum for PEO (Fig. 1), one maximum and one minimum. Moreover, the maxima for different salt contents (Y_S) are close to $Z''/R_b = 0.5$ but not identical to 0.5. This is consistent with $n < 1$, as mentioned above. We also note extreme values shift to higher frequencies with increasing salt content, and the ratio of frequencies to extreme values is quite small; it amounts maximal to order 0 (0.1) for $\omega_{\min}/\omega_{\max}$. In contrast to PEO, one observes for the ENR polymers only a maximum. ENR-25 displays a maximum solely at high salt content, $Y_S > 0.2$, and ENR-50 exhibits the maximum independent of salt content; the latter fact indicates phase separation in ENR-rich and ENR-poor phase [unpublished results].

The two extreme values of Fig. 1 allow for determination of quantity D_{ion} as given in Eq. (4) with the assistance of $l=L \cdot C_f/C_{dl}$. Known quantity D_{ion} in turn allows for the determination of electric active concentration, i.e., C_S after Eq. (3). Accordingly, quantity $D_{\text{ion}} \cdot C_S \propto \sigma_{\text{DC}}$. Concentration C_S as estimated in that way is plotted for PEO in Fig. 2. In contrast to σ_{DC} , which increases by 2 orders of magnitude in the range of

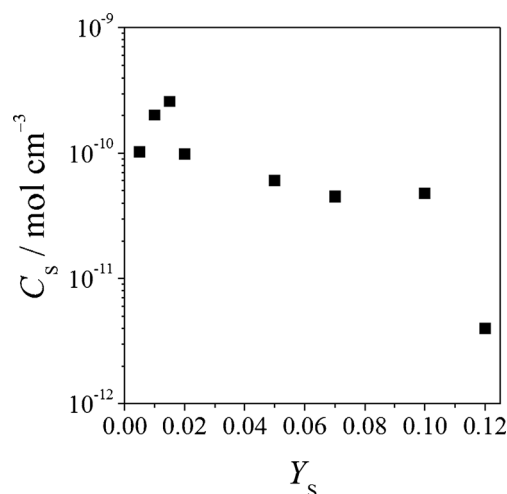


Fig. 2 Electric active carrier concentration C_S in PEO versus salt concentration Y_S determined after Eq. (3) using diffusion coefficient D_{ion} plotted in Fig. 3

Table 2 Data from impedance spectroscopy, transport coefficient, and degree of dissociation

Y_S	$\sigma_{DC}/(\Omega\text{ cm})^{-1}$	$\omega_{\min}/\text{s}^{-1}$	$\omega_{\max}/\text{s}^{-1}$	$D_{\text{ion}}/\text{cm}^2\text{ s}^{-1}$	α	l/m	$C_S/\text{mol cm}^{-3}$
PEO							
0.005	3.5×10^{-9}	690	6,685	9.4×10^{-6}	1.8×10^{-6}	1.2×10^{-6}	1.0×10^{-10}
0.05	4.9×10^{-8}	4,430	34,620	2.2×10^{-4}	2.6×10^{-7}	1.5×10^{-6}	6.0×10^{-11}
0.1	5.3×10^{-7}	62,830	4.72×10^5	3.5×10^{-3}	2.1×10^{-8}	2.4×10^{-6}	4.8×10^{-11}
ENR-25							
0.12	2.8×10^{-9}	-	314	-	-	-	-
0.25	4.2×10^{-7}	310 ^a	8,170	8.2×10^{-7}	6.1×10^{-5}	5.1×10^{-7}	1.4×10^{-7}
ENR-50							
0.1	1.4×10^{-8}	258 ^a	5,340	1.2×10^{-6}	3.7×10^{-6}	6.8×10^{-7}	3.4×10^{-9}
0.2	2.7×10^{-8}	245 ^a	5,270	9.7×10^{-7}	3.8×10^{-6}	6.3×10^{-7}	6.9×10^{-9}

^a Data estimated after procedure given in the “Appendix” section

added salt amount Y_S , concentration C_S stays roughly constant in that range. Hence, ascent of σ_{DC} is coined by increase in quantity D_{ion} . As a consequence of Fig. 2, degree of dissociation after Eq. (5) decreases with ascending concentration Y_S of salt in the polymer electrolyte system. Examples are summarized in Table 2 and plotted versus salt content Y_S in Fig. 3.

In contrast to quantity C_S , quantity D_{ion} of PEO increases with increasing concentration Y_S . This result is dominantly governed by ascending frequency ω_{\min} (cf. Eq. (14)). Moreover, one may relate diffusion coefficient to friction coefficient (ζ) by $D_{\text{ion}} = k_B T / \zeta$. For qualitative discussion, we adopt Stokes formulation of friction coefficient, $\zeta = 6\pi\eta r$, where η denotes viscosity of the polymer and r stands for the size of the charge carrier. Several experiments proved that viscosity of polymer melts increases when salt is added. Hence, we learn from the increase of D_{ion} in Fig. 3a that the size of the diffusing charge carriers dramatically decreases with increasing salt content. In other words, the “solvation” of ions by segments of PEO decreases with ascending salt content. This observation illustrates the fact that segments, which are not

actively participating in the dynamics, render ionic transport properties robust against geometric perturbations. Under dynamic conditions, structure formation of ions and segments diminishes with increasing salt content.

Only mixtures with PEO exhibit effects in the experimentally accessible DC limit that are due to double-layer capacitor. Minima in imaginary parts of impedance cannot be monitored in polymer electrolytes with rubbers. As a result, diffusion coefficient and degree of dissociation are determined directly only for PEO; whereas for the rubbers, we have to approximate them as given in the “Appendix” section (cf. Eq. (16)). DC conductivity of ENR-25 is low in the order of 10^{-10} to $10^{-9} (\Omega\text{ cm})^{-1}$, up to high salt content. One observes a jump by 2 orders of magnitude only for $Y_S > 0.2$ [13]. Therefore, Fig. 3 shows only diffusion coefficient and degree of dissociation for two relatively high salt contents. Analog figures to Fig. 1 for ENR-50 display coincidence of Z'/R_b for different values Y_S , that is these quantities do not vary with salt content. As a result, diffusion coefficient and degree of dissociation stay constant over a wide range of salt concentration. This is reflected fairly in Fig. 3.

Fig. 3 Transport properties of charge carriers versus salt content Y_S in polymer electrolytes. Filled squares indicate PEO, triangles are ENR-50, stars indicates ENR-25. (a) Diffusion coefficient D_{ion} after Eq. (17), (b) degree of dissociation α after Eq. (5)

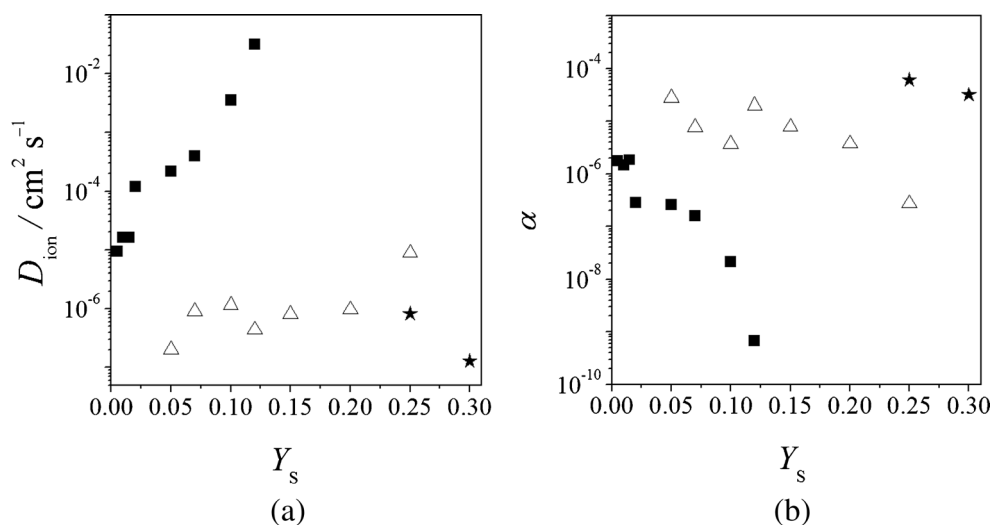


Fig. 3b presents degrees of dissociation as calculated after Eq. (5) with diffusion coefficient D_{ion} after Eq. (17). Decrease of degree of dissociation is characteristic for PEO. The same tendency has been observed in low-molecular electrolytes where ion-pair formation takes place with increasing salt concentration. We point here towards interplay between densities of charge carriers or degree of dissociation α and transport characterized by coefficient D_{ion} . High diffusion coefficients, supported by short relaxation times (τ_{min}), cause DC conductivity to be high. Contrary to concentration of charge carriers which has minor effect only.

We note that the thickness of double layer stays roughly constant with increasing salt content in PEO whereas the diffusion coefficient markedly ascends. This is consistent with increasing conductivity and descending density of charge carriers or degree of dissociation. In ENR, one observes a high degree of dissociation, but only a low diffusion coefficient. The result agrees with low values of DC conductivity, at low Y_S , for the ENRs listed in Table 2. Rough constancy of both diffusion coefficient and degree of dissociation for ENR-50 are in agreement with the discussion before.

We add a few words about length l introduced with Eq. (4). High diffusion coefficient D_{ion} makes possible enlarged length l . One finds $l = 1.2 \cdot 10^{-6}$ m for PEO in the limit of very low salt concentration (cf. Table 2). This result agrees in order of magnitude with Debye length, $1.6 \cdot 10^{-6}$ m, when calculated with corresponding concentration C_S . Thickness L of the samples used in the experiments was in the order of 10^{-3} m. Hence, we get for $l/L = O(10^{-3})$, which gives also the order of C_f/C_{dl} after Eq. (12).

Conclusion

Poly(ethylene oxide) (PEO) and epoxidized natural rubber (ENR) with addition of lithium perchlorate (LiClO_4) were studied. Impedance relaxation was investigated at room temperature over a wide range of salt concentration. Subject matter of the paper is the variation of transport properties and degree of dissociation of LiClO_4 in polymer with salt content. The imaginary part of impedance exhibits two extreme frequencies that rule properties in the DC limit. Therefore, impedance data serve for the determination of transport properties and degree of dissociation of salt in polymer.

Acknowledgments The authors gratefully acknowledge Assoc. Prof. Dr. Lar Har Sim, Siti Nor Hafiza Mohd Yusoff, and Amirah Hashifudin for the complex impedance data for ENR and PEO, which were used in this paper. This work is supported by fundamental research grants [600-RMI/FRGS 5/3(67/2013)] provided by the Ministry of Education.

Appendix

Influence of double-layer capacitor, diffusion coefficient, and degree of dissociation

When the double-layer capacitor C_{dl} is not negligible at low frequencies and no dispersion of relaxation time occurs, the impedance reads

$$\frac{Z}{R} = \frac{1}{1 + i(\omega\tau)} + \frac{1}{i(\omega\tau)} \frac{2C_f}{C_{\text{dl}}} \quad (8)$$

where parameter τ is given by Eq. (2), $\tau = \omega_{\text{max}}^{-1}$ when $C_f/C_{\text{dl}} = 0$. The imaginary part of Eq. (8) displays a function of frequency of two extreme values at ω_{max} and ω_{min} . These values are solutions of the following equation:

$$x^2(1-x^2) = A(1+x^2)^2 \quad \text{with } x \equiv \omega\tau \quad A \equiv 2 \frac{C_f}{C_{\text{dl}}} \quad (9)$$

It results

$$x_{\text{min}}^2 = \frac{1}{2(1+A)} \left[(1-2A) - \sqrt{1-8A} \right] \quad (10)$$

and the analogous expression for x_{max} .

For the determination of A , one may use the following approximations:

I. When the two extreme values are sufficiently distant from each other, we may use in Eq. (9) the approximation $1 \approx \omega_{\text{max}}\tau$. Quantity A is then given by ratio $(\omega_{\text{min}}/\omega_{\text{max}})^2$

$$\frac{2C_f}{C_{\text{dl}}} = \left(\frac{\omega_{\text{min}}}{\omega_{\text{max}}} \right)^2 \frac{1 - \left(\frac{\omega_{\text{min}}}{\omega_{\text{max}}} \right)^2}{\left[1 + \left(\frac{\omega_{\text{min}}}{\omega_{\text{max}}} \right)^2 \right]^2} \approx \left(\frac{\omega_{\text{min}}}{\omega_{\text{max}}} \right)^2 \quad (11)$$

The last approximation follows since $(\omega_{\text{min}}/\omega_{\text{max}})^2 \ll 1$. We note that the ratio of capacitors is given by the ratio of corresponding thicknesses, double layer and film thickness, l and L , respectively

$$\frac{C_f}{C_{\text{dl}}} = \frac{l}{L} \quad (12)$$

Knowing the ratio C_f/C_{dl} after Eq. (11) allows easily for determination of diffusion coefficient D_{ion} . It describes random walk of charge carriers. In the DC limit, we have

$$l^2 = D_{\text{ion}}\tau_{\text{min}} \quad (13)$$

with $\tau_{\text{min}} = \omega_{\text{min}}^{-1}$.

Diffusion coefficient: Using Eqs. (12) and (13), we get for diffusion coefficient D_{ion}

$$D_{\text{ion}} = \omega_{\text{min}} L^2 \left(\frac{C_f}{C_{\text{dl}}} \right)^2 \quad (14)$$

II. In the case the minimum shifts to very low frequencies and is not experimentally accessible, we may employ for estimation of A the imaginary part of Eq. (8). It can be recast as follows:

$$\frac{Z''}{R_b} x = A + \frac{x^2}{1 + x^2} \quad (15)$$

One recognizes that the intercept of Zf versus squared frequency, f^2 , reads

$$\text{intercept} = \frac{AR}{2\pi\tau} \quad (16)$$

Time constant τ is approximated again via $\omega_{\text{max}}\tau=1$, and Eq. (10) allows for estimation of ω_{min} .

Degree of dissociation: D_{ion} follows after Eq. (14). The combination with Eq. (3) allows for calculation of concentration C_s . Definition of α in Eq. (5) gives α .

Double-layer capacitor and dispersion of relaxation times

Extension of Eq. (8) to dispersion of relaxation times reads

$$\frac{Z(\omega)}{R} = \frac{1}{1 + (i\omega\tau)^n} + 2 \frac{C_f}{C_{\text{dl}}} \frac{1}{(i\omega\tau)^n} \quad (17)$$

Equation (8) shows that only imaginary part of Z'' is influenced by the ratio of capacitors C_f/C_{dl} . This is not any more true for $n < 1$. We get from Eq. (17)

$$\begin{aligned} \frac{Z'}{R_b} &= \frac{\left[1 + (\omega\tau)^n \cos\left(n\frac{\pi}{2}\right) \right] (\omega\tau)^n + 2N \frac{C_f}{C_{\text{dl}}} \cos\left(n\frac{\pi}{2}\right)}{N(\omega\tau)^n} \\ \frac{Z''}{R_b} &= \frac{(\omega\tau)^{2n} \sin\left(n\frac{\pi}{2}\right) + 2N \frac{C_f}{C_{\text{dl}}} \sin\left(n\frac{\pi}{2}\right)}{N(\omega\tau)^n} \end{aligned} \quad (18)$$

with $N = 1 + 2(\omega\tau)^n \cos\left(n\frac{\pi}{2}\right) + (\omega\tau)^{2n}$.

In the limit of low frequencies, $\omega \rightarrow 0$, it results into Eq. (7).

References

- Armand MB (1986) Polymer electrolytes. *Annu Rev Mater Sci* 16(1):245–261. doi:10.1146/annurev.ms.16.080186.001333
- Berthier C, Gorecki W, Minier M, Armand MB, Chabagno JM, Rigaud P (1983) Microscopic investigation of ionic conductivity in alkali metal salts-poly(ethylene oxide) adducts. *Solid State Ionics* 11(1):91–95. doi:10.1016/0167-2738(83)90068-1
- Agrawal RC, Pandey GP (2008) Solid polymer electrolytes: materials designing and all-solid-state battery applications: an overview. *J Phys D Appl Phys* 41(22):223001–2230018. doi:10.1088/0022-3727/41/22/223001
- Alloin F, D'Apré A, Kissi NE, Dufresne A, Bossard F (2010) Nanocomposite polymer electrolyte based on whisker or microfibrils polyoxyethylene nanocomposites. *Electrochim Acta* 55(18):5186–5194. doi:10.1016/j.electacta.2010.04.034
- Azizi Samir MAS, Alloin F, Gorecki W, Sanchez J-Y, Dufresne A (2004) Nanocomposite polymer electrolytes based on poly(oxyethylene) and cellulose nanocrystals. *J Phys Chem B* 108(30):10845–10852. doi:10.1021/jp0494483
- Chan CH, Kammer HW (2008) Properties of solid solutions of poly(ethylene oxide)/epoxidized natural rubber blends and LiClO_4 . *J Appl Polym Sci* 110(1):424–432. doi:10.1002/app.28555
- Chan CH, Kammer H-W, Sim LH, Nasir NHA, Winie T (2012) On the thermodynamics of solid solutions of polymer and salt. *Polym Eng Sci* 52(11):2277–2284. doi:10.1002/pen.23290
- Idris R, Glasse MD, Latham RJ, Linford RG, Schlindwein WS (2001) Polymer electrolytes based on modified natural rubber for use in rechargeable lithium batteries. *J Power Sources* 94(2):206–211. doi:10.1016/S0378-7753(00)00588-7
- Mark Harry B, Rubinson Judith F (2002) Challenges and opportunities: where do we go from here? In: Rubinson Judith F, Mark Harry B (eds) *Conducting polymers and polymer electrolytes*, vol 832. ACS symposium series, vol ACS symposium series 832. American Chemical Society, Washington, DC, pp 203–204. doi:10.1021/bk-2003-0832.ch015
- Di Noto V, Vittadello M, Yoshida K, Lavina S, Negro E, Furukawa T (2011) Broadband dielectric and conductivity spectroscopy of Li-ion conducting three-dimensional hybrid inorganic–organic networks as polymer electrolytes based on poly(ethylene glycol) 400, Zr and Al nodes. *Electrochim Acta* 57:192–200. doi:10.1016/j.electacta.2011.04.095
- Hallinan DT, Mullin SA, Stone GM, Balsara NP (2013) Lithium metal stability in batteries with block copolymer electrolytes. *J Electrochem Soc* 160(3):A464–A470. doi:10.1149/2.030303jes
- Winie T, Hanif NSM, Chan CH, Arof AK (2014) Effect of the surface treatment of the TiO_2 fillers on the properties of hexanoyl chitosan/polystyrene blend-based composite polymer electrolytes. *Ionics* 20(2):347–352. doi:10.1007/s11581-013-0983-1
- Chan CH, Kammer H-W, Sim LH, Mohd Yusoff SNH, Hashifudin A, Winie T (2014) Conductivity and dielectric relaxation of Li salt in poly(ethylene oxide) and epoxidized natural rubber polymer electrolytes. *Ionics* 20(2):189–199. doi:10.1007/s11581-013-0961-7
- Walter R, Selser JC, Smith M, Bogoslovov R, Piet G (2002) Network viscoelastic behavior in poly(ethylene oxide) melts: effects of temperature and dissolved LiClO_4 on network structure and dynamic behavior. *J Chem Phys* 117(1):427–440. doi:10.1063/1.1481059
- Polo Fonseca C, Cavalcante FJ, Amaral FA, Zani Souza CA, Neves S (2007) Thermal and conduction properties of a PCL-biodegradable gel polymer electrolyte with LiClO_4 , LiF_3CSO_3 , and LiBF_4 salts. *Int J Electrochem Sci* 2:52–63
- Di Noto V, Vittadello M, Lavina S, Fauri M, Biscazzo S (2001) Mechanism of ionic conductivity in poly(ethyleneglycol 400)/

- (LiCl)x electrolytic complexes: studies based on electrical spectroscopy. *J Phys Chem B* 105(20):4584–4595. doi:[10.1021/jp0103934](https://doi.org/10.1021/jp0103934)
17. Berson A, Lindgren J, Huang W, Frech R (1995) Coordination and conformation in PEO, PEGM and PEG systems containing lithium or lanthanum triflate. *Polymer* 36(23):4471–4478. doi:[10.1016/j.bbr.2011.03.031](https://doi.org/10.1016/j.bbr.2011.03.031)
 18. Robitaille CD, Fauteux D (1986) Phase diagrams and conductivity characterization of some PEO-LiX electrolytes. *J Electrochem Soc* 133(2):315–325. doi:[10.1149/1.2108569](https://doi.org/10.1149/1.2108569)
 19. Wieczorek W, Raducha D, Zalewska A, Stevens JR (1998) Effect of salt concentration on the conductivity of PEO-based composite polymeric electrolytes. *J Phys Chem B* 102(44):8725–8731. doi:[10.1021/jp982403f](https://doi.org/10.1021/jp982403f)
 20. Xi J, Qiu X, Zheng S, Tang X (2005) Nanocomposite polymer electrolyte comprising PEO/LiClO₄ and solid super acid: effect of sulphated-zirconia on the crystallization kinetics of PEO. *Polymer* 46(15):5702–5706. doi:[10.1016/j.polymer.2005.05.051](https://doi.org/10.1016/j.polymer.2005.05.051)
 21. Chan CH, Sim LH, Kammer HW, Tan W, Abdul Nasir NH (2011) Ionic transport and glass transition temperature of polyether-salt complexes: dependence on molecular mass of polymer. *Mater Res Innov* 15(1):s14. doi:[10.1179/143307511X13031890747336](https://doi.org/10.1179/143307511X13031890747336)
 22. Mohd Yusoff SNH, Sim LH, Chan CH, Hashifudin A, Kammer H-W (2013) Solid solution of polymer electrolytes based on modified natural rubber. *Polym Res J* 7(2):159–169
 23. Sim LH, Chan CH, Kammer H-W (2011) Selective localization of lithium perchlorate in immiscible blends of poly(ethylene oxide) and epoxidized natural rubber. In: Hamzah MK (ed) IEEE conference on open systems: 2010 international conference on science and social research (CSSR 2010), Kuala Lumpur, Malaysia, 5–7 Dec 2010. IEEE Xplore Digital Library, pp 499–503. doi:[10.1109/CSSR.2010.5773829](https://doi.org/10.1109/CSSR.2010.5773829)
 24. Noor S, Ahmad A, Talib I, Rahman M (2010) Morphology, chemical interaction, and conductivity of a PEO-ENR50 based on solid polymer electrolyte. *Ionics* 16(2):161–170. doi:[10.1007/s11581-009-0385-6](https://doi.org/10.1007/s11581-009-0385-6)
 25. Noor SAM, Ahmad A, Rahman MYA, Talib IA (2009) Preparation and characterization of a solid polymer electrolyte PEO-ENR50 (80/20)-LiCF₃SO₃. *J Appl Polym Sci* 113(2):855–859. doi:[10.1002/app.29951](https://doi.org/10.1002/app.29951)
 26. Noor SAM, Ahmad A, Talib I, Rahman M (2011) Effect of ZnO nanoparticles filler concentration on the properties of PEO-ENR50-LiCF₃SO₃ solid polymeric electrolyte. *Ionics* 17(5):451–456. doi:[10.1007/s11581-011-0534-6](https://doi.org/10.1007/s11581-011-0534-6)
 27. Chan CH, Sim LH, Kammer HW, Tan W (2012) The influence of the amorphous polymer on conductivity, morphologies and thermal properties of polyether-based blends with addition of inorganic salt. *Am Inst Phys Conf Proc* 1455(1):197–207. doi:[10.1063/1.4732492](https://doi.org/10.1063/1.4732492)
 28. Sim LH, Gan SN, Chan CH, Kammer HW, Yahaya R (2013) Effect of polyacrylate and LiClO₄ on the isothermal crystallization kinetics of PEO. *Progress Polym Res* 1:1–6
 29. Fadzallah IA, Majid SR, Careem MA, Arof AK (2014) Relaxation process in chitosan–oxalic acid solid polymer electrolytes. *Ionics* 20(7):969–975. doi:[10.1007/s11581-013-1058-z](https://doi.org/10.1007/s11581-013-1058-z)
 30. Sim LH, Gan SN, Chan CH, Kammer HW, Yahaya R (2013) Conductivity studies of a chitosan-based polymer electrolyte. *Phys B Condens Matter* 373(1):23–27
 31. Gelling IR (1987) Epoxidized natural rubber. *Natl Rubber Technol* 18:21–29
 32. Sim LH, Chan CH, Kammer HW (2011) Melting behaviour, morphology and conductivity of solid solutions of PEO/PAC blends and LiClO₄. *Mater Res Innov* 15(1):s71–s74. doi:[10.1179/143307511X13031890747895](https://doi.org/10.1179/143307511X13031890747895)
 33. Sim LH, Gan SN, Chan CH, Kammer HW, Yahya R (2009) Compatibility and conductivity of LiClO₄ free and doped polyacrylate - poly(ethylene oxide) blends. *Mater Res Innov* 13(3):278–281. doi:[10.1179/143307509X440523](https://doi.org/10.1179/143307509X440523)